Performance of the CLD detector for FCC-ee

Oleksandr Viazlo (CERN)
on behalf of the FCC and CLICdp collaborations

FCC week 2019, Brussels

26 June 2019

Update of performance studies of the CLD detector

- Full detector simulation and reconstruction is done with iLCSoft
- Geometry description with DD4hep package
- Reconstruction framework Marlin
- Tracking with conformal tracking and particle-flow reconstruction with PandoraPFA

Content

- Overview of the CLD detector model
- Beam-induced backgrounds
- Tracking performance
- Particle flow event reconstruction performance
- Further detector optimization
- Summary

CLD detector model

- Overview
- Tracking system
- Calorimeter

CLD detector model

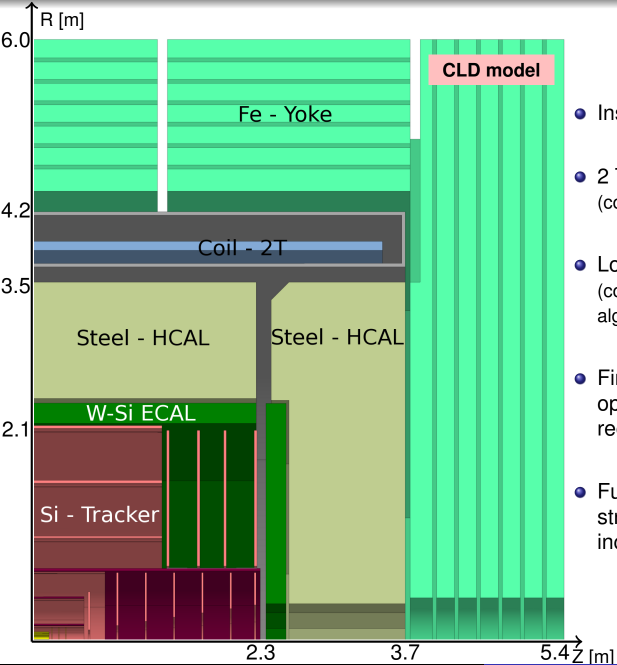

- Inspired by CLICdet design
- 2 T magnetic field
  (constraint from the machine)
- Low mass vertex and tracker
  (conformal tracking as the main tracking algorithm)
- Fine-grained ECAL and HCAL optimized for particle flow reconstruction
- Full detector simulation with support structures, cables and services included in the model

Tracking system

Vertex detector

- Silicon pixels: 25x25μm^2
- Single-point resolution: 3 μm
- 3 double layers in barrel: r = 17, 37, 57 mm
- 3 double endcap disks per side: z = 160, 230, 300 mm
- Material budget: 0.6% X_0 per double layer

Tracker detector

- Silicon pixel and microstrips detector
- Inner Tracker:
  - 3 barrel layers, 7 disks per side
- Outer Tracker:
  - 3 barrel layers, 4 disks per side
- Single-point resolution:
  - 7 μm x 90 μm
  - except 1st IT disk: 5 μm x 5 μm
- Material: 1.1-1.6% X_0 per layer

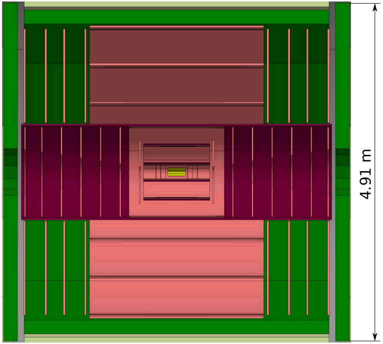

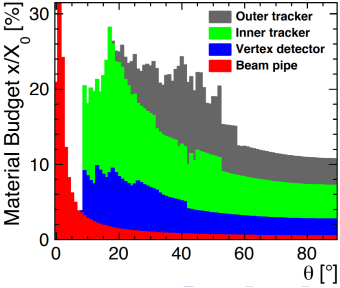

Electromagnetic Calorimeter

- Si-W sampling calorimeter
- cell size 5x5 mm^2
- 40 layers (1.9 mm thick W plates)
- Depth: 22 X_0, 1 λ_I, 20 cm

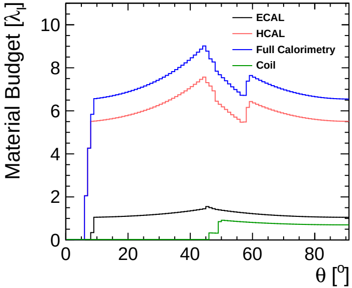

Hadronic Calorimeter

- Scintillator-steel sampling calorimeter
- cell size 30x30 mm^2
- 44 layers (19 mm thick steel plates)
- Depth: 5.5 λ_I, 117 cm (inspired by ILD)

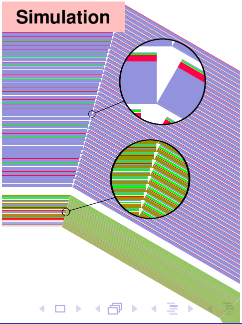

Beam-induced backgrounds

in tracking system

in calorimetry system

- Synchrotron radiation
  - Appropriate masking stops SR photons from hitting the central beam pipe
  - Small effect
- Beamstrahlung induced backgrounds
  - Incoherent e^+e^- pair production
  - $\gamma\gamma \rightarrow$ hadrons (small effect)
- Beam-gas interactions and radiative Bhabhas
  - expected to have small effect

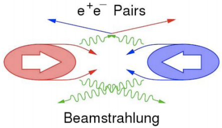

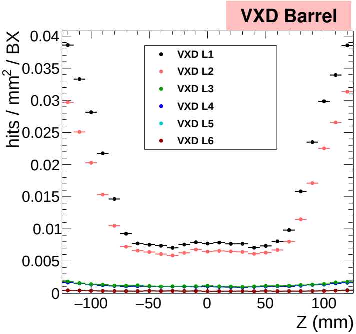

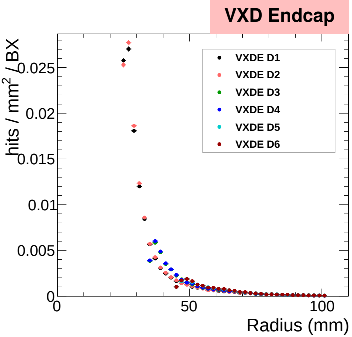

- The energy from incoherent pairs deposited in the ECAL and HCAL
- Has been studied as a function of z in the barrel and as function of radius in the endcap

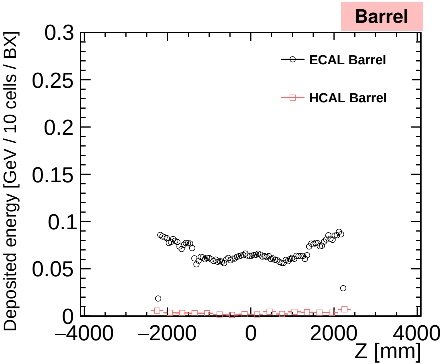

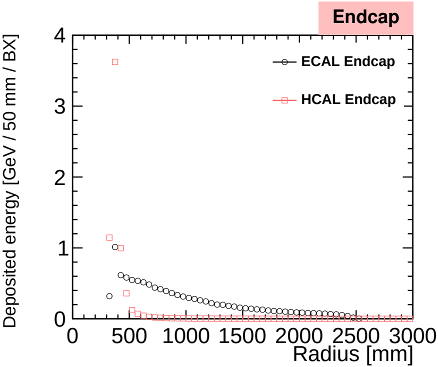

- Energy deposits reach up to 0.1 GeV / 10 cells in ECAL Barrel and 4 GeV / 50 mm in HCAL Endcap

Tracking performance

- with isolated particles
- in complex events
- flavour tagging

Tracking performance with isolated particles

- Performance studies have been done with conformal tracking
  (pattern recognition algorithm developed for ultra-low mass tracking systems)
- Tracking performance with isolated muons:
  - resolution calculated as width of the Gaussian fit of the residual distribution

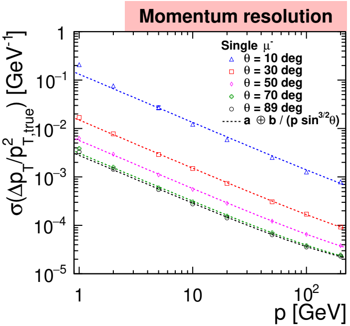

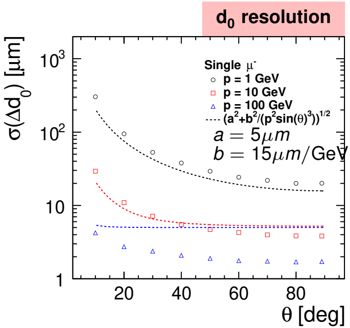

- Transverse momentum resolution: $\approx 7\times10^{-5}\text{GeV}^{-1}$ for 45 GeV muons in barrel
  $\rightarrow$ 125-150 MeV accuracy on muon momentum
- Achieved desired transverse impact resolution:
  $a = 5\mu m$, $b = 15\mu m/\text{GeV}$ (dashed line on right plot)

- Effect on d_0 resolution with different vertex detector layout

+50% of VTX material budget

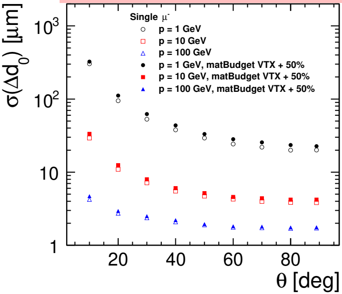

variation of single point resolution

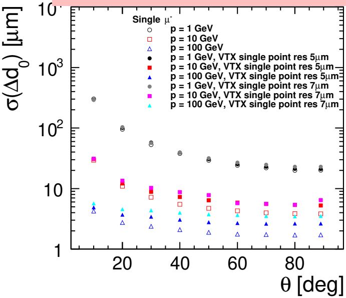

- Mild impact with +50% increase of vertex detector material budget
- Strong correlation of d_0 resolution with single-point resolution particularly at high momenta

- Tracking efficiency with isolated prompt and displaced muons:
  - efficiency = fraction of reconstructed particles out of the reconstructable
  - reconstructable particle:
    - $p_T > 0.1$ GeV
    - $|\cos\theta| < 0.99$
    - $\#$ unique hits: 4 for prompt; 5 for displaced tracks

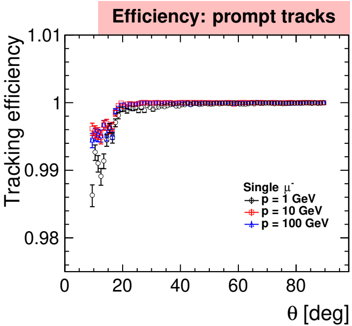

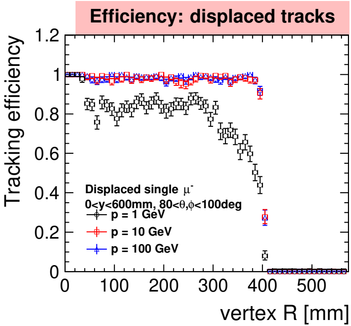

- Tracking is fully efficient starting from $\sim 10^\circ$
- Tracking algorithm successfully reconstructs displaced tracks:
  - sharp drop at $\sim$400 mm corresponds to position of 8-th silicon layer $\rightarrow$ not enough hits for track reconstruction (5 hits per track is required)

- Tracking efficiency with light flavour di-jets $Z \rightarrow q\bar{q}$ ($q = u, d, s$) with and without beam induced background:
  - additional requirement on track purity $> 75\%$
  - purity = $\#$hits left by MC particle / $\#$hits in track

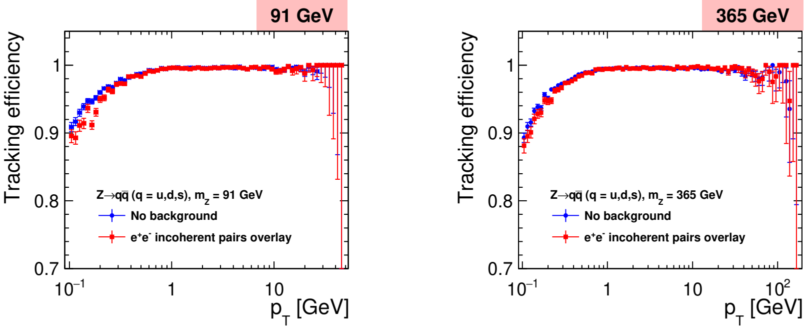

- Tracking is fully efficient from $p_T \approx 500$ MeV
- > 90 % efficiency for low momentum tracks (p_T = 100 - 500 MeV)
- Robustness against beam background both at 91.2 and 365 GeV

Tracking performance in complex events

- Tracking efficiency with di-jets $Z \to b\bar{b}$:
  - fake rate = the fraction of reconstructed tracks with purity $< 75\%$
  - purity = #hits left by MC particle / #hits in track

Efficiency

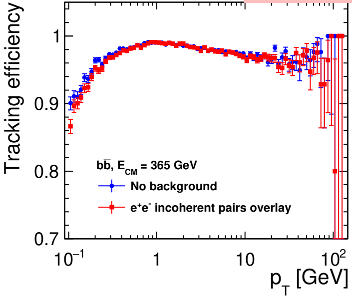

Fake rate

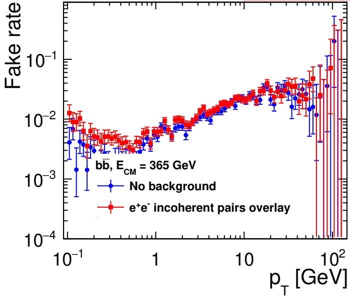

- High reconstruction efficiency with per cent level of fake rate
  - Slight degradation of efficiency at higher energies $\to$ additional tuning of algorithm parameters is needed
- The effect of the background is negligible

- Heavy-flavour tagging efficiency for forward region ($\theta = 30^\circ$):
  - comparison of tagging efficiencies with using conformal and truth tracking
  - truth tracking = assuming perfect pattern recognition

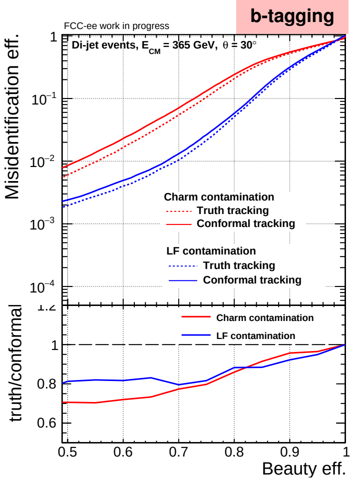

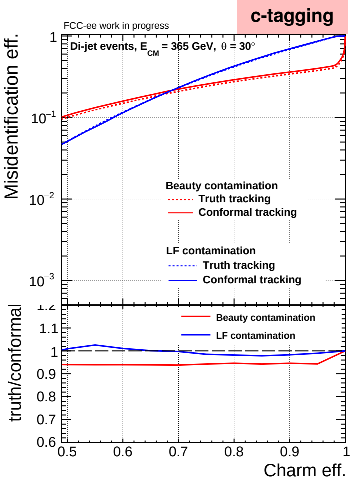

- b-tagging at 80% eff.: $\approx$ 20% miss-id. for c and $\approx$ 5% for light flavour
- c-tagging at 80% eff.: $\approx$ 25% miss-id. for b and $\approx$ 40% for light flavour
- Some deviation between truth and conformal tracking $\rightarrow$ work is ongoing

Particle flow event reconstruction performance

→ jet energy resolution

→ W-Z mass peak separation

- Event reconstruction is done with PandoraPFA particle flow package
- JER is studied with di-jet events using $Z \to q\bar{q}, (q = u, d, s)$ at $\sqrt{s} = 91.2 - 365$ GeV
  - JER is calculated as the energy sum of all reconstructed particles
  - RMS90 is defined as the RMS in the smallest range of the reconstructed energy containing 90% of the events

JER vs cos(θ)

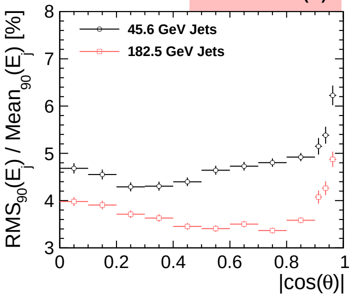

JER vs jet energy

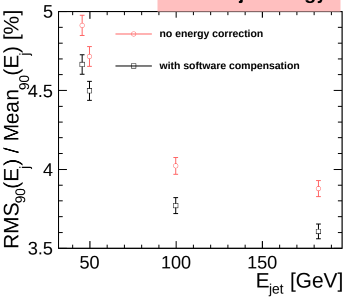

- Jet Energy Resolutions:
  - 45.6 GeV jets: 4-5 %
  - 182.5 GeV jets: 3-4 %
- Software compensation (energy regularization technique for fine-grained calorimeters) improves results by up to 10%

Jet Energy Resolution with background overlaid

- Jets are reconstructed with Valencia clustering algorithm ($\Delta R = 1.1$) in two-jet exclusive mode
- Assuming 400 ns integration time window

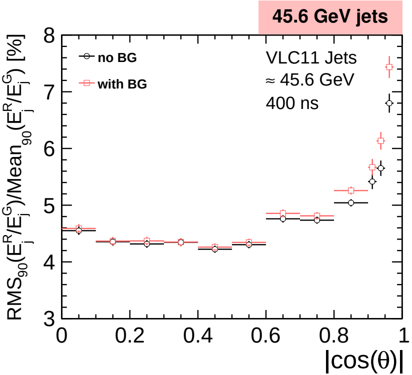

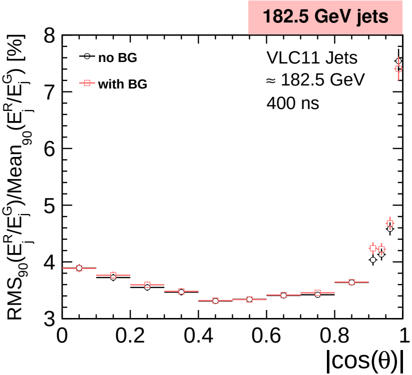

- overall the impact of the background is negligible at both centre-of-mass energies
- except in the forward region at 91.2 GeV, where the relative energy deposits from background particles is the largest
- no timing or p_T cuts were applied

The angular resolution of jets

- The angular resolution of jets has been studied by comparing azimuthal ϕ and polar θ angles of reconstructed and particle level jets

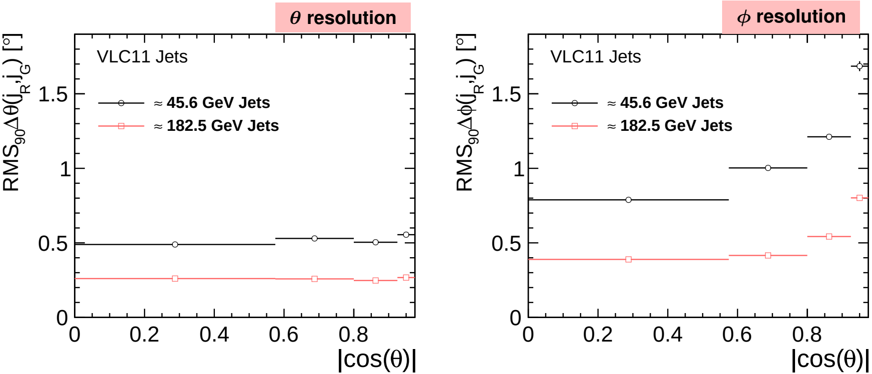

- The ϕ resolution for jets is worse than the θ resolution due to the effect of the magnetic field
- Degradation of the ϕ resolution with $\cos(\theta)$ can be explained with detector granularity

- Study of the ability to distinguish hadronic decays of W- and Z-bosons
- Two processes of interest: $WW \rightarrow \mu\nu_\mu qq$ and $ZZ \rightarrow \nu\nu qq$ (250 GeV)
  - decay products from leptonic decays of bosons are excluded from the jet reconstruction

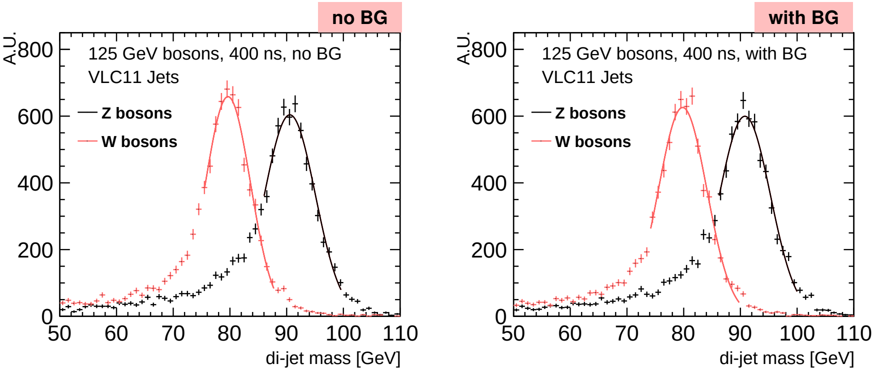

- Invariant W and Z mass peaks are iteratively fitted with a Gaussian in the range $[\mu - \sigma, \mu + 2\sigma]$ until σ of the fit stabilizes within $\pm 5\%$
- Fit is also done with 365 GeV background overlaid (right plot)

W-Z Mass Peak Separation

- The separation power is calculated from the fit parameters as:
  $(m_Z - m_W)/\sigma_{average}$ (where $\sigma_{average} = (\sigma_Z + \sigma_W)/2$)
- The separation power is calculated using two different methods:
  - the mass of W- and Z-boson is obtained as the mean of the Gaussian fit
  - the mass distributions are scaled such that the mean of the fit becomes equal to the PDG values of the W- and Z-boson mass.

background overlay	ΔR	$\sigma_{m(W)}/m(W)$ [%]	$\sigma_{m(Z)}/m(Z)$ [%]	Separation [σ]	Separation (fixed mean) [σ]
no BG	0.7	5.94	5.75	2.19	2.16
with BG	0.7	5.95	5.9	2.13	2.13
no BG	0.9	5.26	5.11	2.46	2.43
with BG	0.9	5.18	5.19	2.43	2.43
no BG	1.1	4.99	4.94	2.58	2.54
with BG	1.1	5.36	4.96	2.5	2.45

- small effect from the background
- CLD detector provides 2.5σ W- and Z-bosons mass peak separation power

Further detector optimization

→ ECAL optimization study

→ effect of central beam pipe diameter reduction

- Initially ECAL was adopted from CLICdet model without modification of the layer numbers, cell size, etc.
- Longitudinal segmentation with 40 identical Si-W layers is required for excellent energy resolution for high energy photons which is an important requirement for CLIC program
- Investigate effect of reducing number of layers to 30 keeping a constant depth of ECAL about 22 X_0 (increase thickness of W plates from 1.9 mm to 2.35 mm)

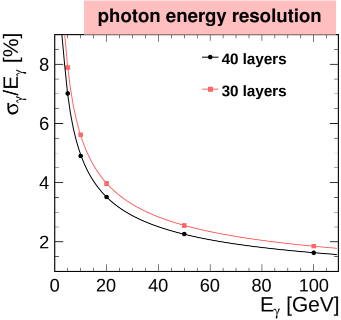

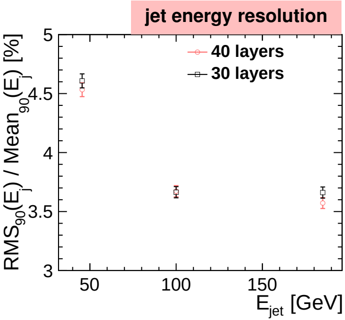

- Photon (ECAL) resolution:
  - 40 layers: $\frac{\sigma_{EM}}{E} = \frac{15.6\%}{\sqrt{E}} \oplus 0.5\%$
  - 30 layers: $\frac{\sigma_{EM}}{E} = \frac{17.6\%}{\sqrt{E}} \oplus 0.6\%$

Flavour tagging efficiencies: smaller beam pipe

- Investigate detector performance with a smaller beam pipe radius (15 mm $\rightarrow$ 10 mm)
- New detector model with vertex detector layout adjusted to smaller beam pipe (FCCee_o1_v04 - reference det. model; FCCee_o2_v01 - model with smaller beam pipe)

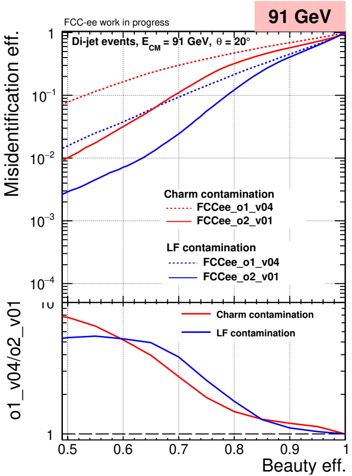

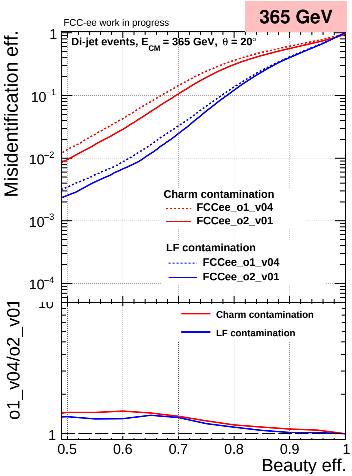

- Study is presented in the talk by E. Leogrande (27 Jun, FCC-ee MDI session)

Full simulation studies demonstrate excellent performance of the CLD detector with:

- Fully efficient tracking starting from 500 MeV
- Excellent jet energy resolution (3-5 %) and 2.5σ W- and Z-bosons mass peak separation power
- No significant effect on performance from beam-induced background
- Promising flavour tagging detector capabilities

Ongoing studies and plans

- Detector performance with reduced beam pipe diameter
- ECAL layout optimization
- Possibilities of more compact tracker
- Increase ECAL forward coverage
- Detector-MDI integration studies

Thank you for your attention!

BACKUP

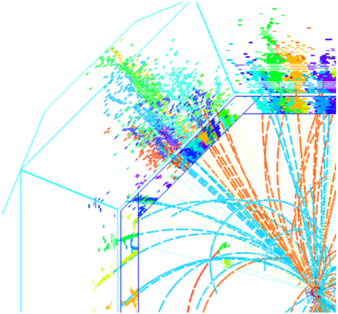

- Average jet composition: to measure with:
  60% charged particles → tracker
  30% photons → ECAL
  10% neutral hadrons → HCAL
- Total jet energy uncertainty:

$$\sigma_{jet} = \sqrt{\sigma^2_{track} + \sigma^2_{ECAL} + \sigma^2_{HCAL} + \sigma^2_{confusion}}$$

- High granularity of calorimeter allows to reduce σ_{HCAL} and $\sigma_{confusion}$

σ_{HCAL}

- Response of el.-m. component of hadron shower in HCAL is different than of hadronic component
  → el.-m. component of shower is denser
- Use local energy density to correct for difference in responses between shower components
  → Software compensation technique (developed by CALICE collaboration)

$\sigma_{confusion}$

- Sophisticated software to identify energy deposits from each particle w/o confusing energies among particles
- PandoraPFA uses $\sim$ 70 algorithms
  - address different topologies
  - correct identification
  - avoid accidental splitting and merging of particles

Comparison of RMS90 and double-sided Crystal Ball fit methods

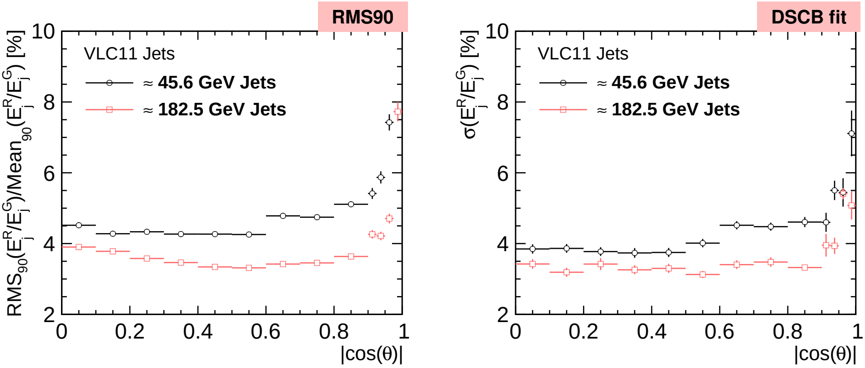

- Overall, the two methods give comparable results, with the RMS90 method yielding slightly more conservative values at low energy

- Fine grain calorimeters with high segmentation to achieve best possible performance of particle flow identification:
  - PandoraPFA algorithms matching information of all detector subsystems to identify and reconstruct each particle correctly by its type: charged hadrons (assigned type: $\pi\pm$), muons, electrons, photons, neutral hadrons (assigned type: neutrons)
  - The main objective of Pandora algorithm is to achieve very excellent jet energy resolution, needed to achieve the desired precision involving hadronic final states

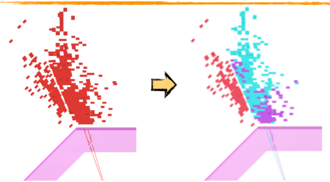

1. Multiple tracks associated to single cluster – split cluster.

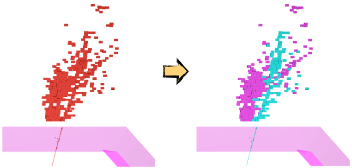

2. Cluster energy much greater than track momentum – split cluster.

- The energy from incoherent pairs deposited in the ECAL and HCAL
- Has been studied as a function of z in the barrel and as function of a radius in the endcap

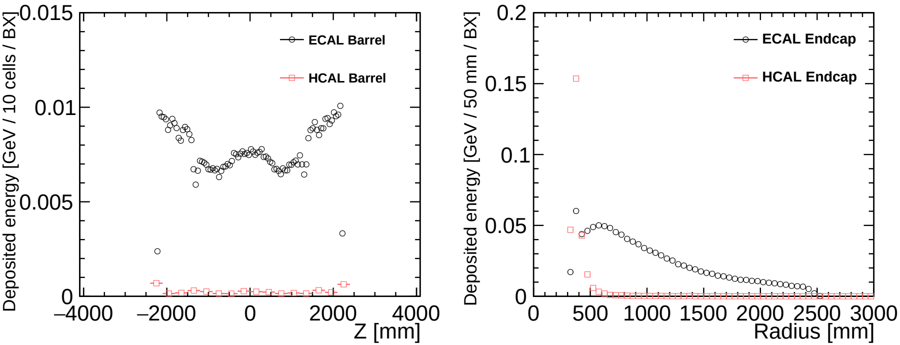

- Assuming 20 BX (400 ns) integration time window at 91.2 GeV
- Energy deposits reach up to 0.2 GeV / 10 cells in ECAL Barrel and 3 GeV / 50 mm in HCAL Endcap

- Efficiency = fraction of matched reconstructed particles out of the simulated MC particles:
  - reconstructed particle of the same type as simulated MC particle
  - angular matching: $\Delta\theta < 1$ mrad and $\Delta\phi < 2$ mrad
  - energy matching:
    - charged particles: $|p_T^{truth} - p_T^{PFO}| < 5\%\ p_T^{truth}$
    - photons: $\Delta E < 5 \times \sigma(\mathrm{ECal}) \approx 0.75 \times \sqrt{E}$

Sample: single particles with flat $\cos(\theta)$ distribution and fixed energy

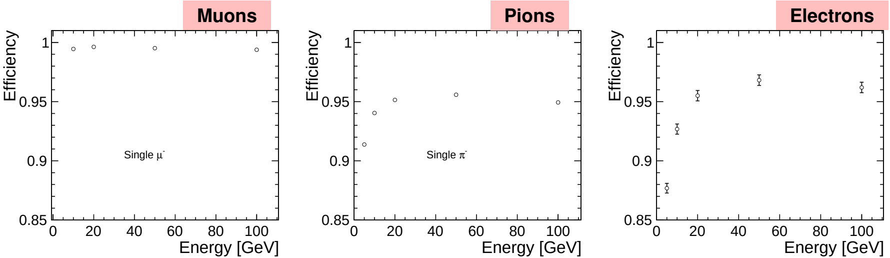

- $>99\%$ muon efficiency and 93-97% pion and electron efficiency for E$>$10 GeV
- Pion inefficiency at high energies is caused by pions being mis-reconstructed as muons
- Electron inefficiency is caused by Bremsstrahlung

- The signatures for unconverted and converted photons are considered separately
- Photon merging procedure is used to recover inefficiency due to photon conversion

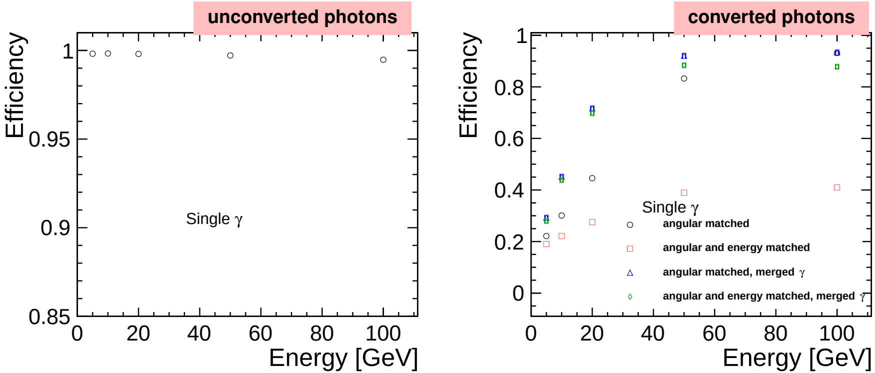

- $>$ 99% efficiency for unconverted photons
- $>$ 90% for $>$50 GeV converted photons
- Further optimization may improve these numbers

VTX and Tracker Layout